THE JOURNAL OF BIOLOGICAL CHEMISTRY VOL. 288, NO. 1, pp. 737–746, January 4, 2013

Heparin Oligosaccharides Inhibit Chemokine (C*X*C Motif) Ligand 12 (CXCL12) Cardioprotection by Binding Orthogonal to the Dimerization Interface, Promoting Oligomerization, and Competing with the Chemokine (C*X*C Motif) Receptor 4 (CXCR4) N Terminus*[S]

Received for publication, June 20, 2012, and in revised form, November 5, 2012 Published, JBC Papers in Press, November 12, 2012, DOI 10.1074/jbc.M112.394064

Joshua J. Ziarek[‡], Christopher T. Veldkamp[§], Fuming Zhang[¶], Nathan J. Murray[‡], Gabriella A. Kartz[‖], Xinle Liang[¶], Jidong Su[‡], John E. Baker[‡], Robert J. Linhardt[¶], and Brian F. Volkman[‡1]

From the Departments of [‡]Biochemistry and [‖]Pharmacology and Toxicology, Medical College of Wisconsin, Milwaukee, Wisconsin 53226, the [§]Department of Chemistry, University of Wisconsin-Whitewater, Whitewater, Wisconsin 53190, and the [¶]Departments of Chemical and Biological Engineering, Chemistry and Chemical Biology, Biology, and Biomedical Engineering and the Center for Biotechnology and Interdisciplinary Studies, Rensselaer Polytechnic Institute, Troy, New York 12180

Background: GAG/CXCL12 interactions are critical for chemokine function but co-administration may abrogate their individual cardioprotective effects in a clinical setting.
Results: Biophysical studies distinguish CXCL12 residues involved in dimerization from those likely to contact heparin directly.
Conclusion: CXCL12 dimerization is required for high affinity heparin binding and protects N-terminal degradation.
Significance: Knowledge of the GAG-binding site will enable future development of heparin-insensitive CXCL12 therapeutics.

The ability to interact with cell surface glycosaminoglycans (GAGs) is essential to the cell migration properties of chemokines, but association with soluble GAGs induces the oligomerization of most chemokines including CXCL12. Monomeric CXCL12, but not dimeric CXCL12, is cardioprotective in a number of experimental models of cardiac ischemia. We found that co-administration of heparin, a common treatment for myocardial infarction, abrogated the protective effect of CXCL12 in an *ex vivo* rat heart model for myocardial infarction. The interaction between CXCL12 and heparin oligosaccharides has previously been analyzed through mutagenesis, *in vitro* binding assays, and molecular modeling. However, complications from heparin-induced CXCL12 oligomerization and studies using very short oligosaccharides have led to inconsistent conclusions as to the residues involved, the orientation of the binding site, and whether it overlaps with the CXCR4 N-terminal site. We used a constitutively dimeric variant to simplify the NMR analysis of CXCL12-binding heparin oligosaccharides of varying length. Biophysical and mutagenic analyses reveal a CXCL12/heparin interaction surface that lies perpendicular to the dimer interface, does not involve the chemokine N terminus, and partially overlaps with the CXCR4-binding site. We further demonstrate that heparin-mediated enzymatic protection results from the promotion of dimerization rather than direct heparin binding to the CXCL12 N terminus. These results clarify the structural basis for GAG recognition by CXCL12 and lend insight into the development of CXCL12-based therapeutics.

Cardiovascular disease is the leading cause of death in the United States, and greater than 50% of these fatalities are asymptomatic (1). The lack of warning for acute cardiovascular injuries, such as myocardial infarctions, underscores the need for highly effective clinical therapeutics. To reduce the possibility of thrombosis at the site of infarction, the American College of Cardiology and the American Heart Association recommend the administration of anticoagulant drugs, such as heparin, during medical treatment for myocardial infarctions (2). Heparin actuates antithrombin, which then inactivates proteins in the coagulation pathway (3). Heparin is not a single molecule but rather describes a family of glycosaminoglycans (GAGs)[2] with specific polysaccharide components of varying length and sulfation. The most common formulations in clinical use are unfractionated heparin and low molecular weight heparin. The molecular mass of unfractionated heparin is typically between 5 and 30 kDa, whereas low molecular weight heparin is usually 1–8 kDa (1). Endogenously, heparan sulfate, structurally related to heparin, is intrinsic to the cell migration properties of chemokines, a family of ~50 structurally homologous *chemo*tactic cyto*kines*.

Chemokines induce the migration of cells by activating G protein-coupled receptors. The direction of chemotaxis is

* This work was supported, in whole or in part, by National Institutes of Health Grants AI058072, GM097381, and AI063325 (to B. F. V.); 1-R15CA159202-01 (to C. T. V.); GM38060 and HL62244 (to F. Z. and R. J. L.); and HL54075 and AI080363 (to J. E. B.). This work was also supported by a postdoctoral fellowship from the Medical College of Wisconsin Cancer Center (to J. J. Z.) and a predoctoral fellowship from the American Heart Association (to G. A. K.).
[S] This article contains supplemental Figs. S1–S8.
[1] To whom correspondence should be addressed: Dept. of Biochemistry, Medical College of Wisconsin, Milwaukee, WI 53226. Tel.: 414-955-8400; Fax: 414-955-6510; E-mail: bvolkman@mcw.edu.

[2] The abbreviations used are: GAG, glycosaminoglycan; DPPIV, dipeptidyl peptidase-IV; TOCSY, total correlation spectroscopy; dp, degree of polymerization; HSQC, heteronuclear single quantum coherence; SPR, surface plasmon resonance.

encoded in a concentration gradient; secreted chemokines are immobilized, by the heparan sulfate GAG chains of proteoglycans, along the endothelial surface. This establishes a gradient with the highest concentrations closest to the origin of secretion (4–6). Originally recognized as the major promoter of leukocyte trafficking, chemokines have been found to participate in a variety of developmental and housekeeping roles, including lymphopoiesis, myelopoeisis, embryogenesis (7), angiogenesis (8), cardiogenesis (9), neuron migration, and cerebral development (10, 11).

Following myocardial ischemia/reperfusion injury, there is increased expression of the chemokine CXCL12 (SDF-1) in cardiac myocytes, endothelial cells, smooth muscle cells, and fibroblasts (12–14). CXCL12 possesses cardioprotective properties when administered either pre- or post-ischemia including reduced infarct zone, decreased scar tissue, increased angiogenesis, resistance to hypoxia/reoxygenation damage, and improved cardiac function (12–19). Despite functional analyses *in vitro* and *in vivo*, the mechanism of CXCL12-induced cardioprotection is disputed: CXCL12 may act through direct activation of growth and survival signaling pathways in cardiomyocytes (12, 13) and/or enhance cardiac regeneration by recruiting hematopoietic stem and endothelial progenitor cells into the heart (18, 20–24).

Although there is ambiguity regarding the cardioprotective mechanism, researchers are aggressively pursuing therapies as evidenced by numerous methods for chemokine administration to ischemic tissue. These include: CXCL12 attached to poly(ethylene glycol)-fibrin patches (18), intravenously introducing self-assembling nanofibers with a timed chemokine release mechanism (15), and injection of viruses engineered to produce protein (21). In each case, CXCL12 treatment is effective, but variations in protection may be related to stability, dosage, or drug interactions. We recently demonstrated that CXCL12 is cardioprotective over a narrow concentration range, whereas a constitutively dimeric form of the chemokine exerts little to no effect (19). Because heparin is commonly administered in response to myocardial infarctions (2) and induces CXCL12 dimerization (25, 26), we hypothesized that the protective properties of CXCL12 may be attenuated by interactions with soluble heparin in a modern clinical setting.

The vital role of GAG binding in CXCL12-directed migration has motivated a series of studies, but its impact on chemokine activity, stability, and receptor interactions remains poorly defined. CXCL12 recognition by heparin oligosaccharides has been characterized using mutagenesis, *in vitro* binding assays, NMR, crystallography, and molecular modeling (27–31). We showed previously that heparin disaccharides bind preferentially to the CXCL12 dimer (26), and others have proposed a binding mode localized to the dimer interface (27, 28). Consequently, we speculated that mutations previously used to define the binding site might reduce heparin affinity indirectly by limiting dimerization.

Using the previously described preferentially monomeric ($CXCL12_{H25R}$) and constitutively dimeric ($CXCL12_2$) variants, we examined the affinity of distinct CXCL12 oligomers for heparin oligosaccharides of varying length. To deconvolute chemical shift perturbations caused by heparin binding from those reporting on dimerization, we monitored oligosaccharide binding to the $CXCL12_2$ dimer by two-dimensional NMR. Heparin-induced chemical shift changes and mutagenesis of basic side chains was used to further refine the GAG binding interface. Binding studies with a CXCR4 N-terminal peptide demonstrate partial overlap and competition with the heparin interface. In contrast to previous reports that heparin binding to Lys-1 protects CXCL12 from cleavage by dipeptidyl peptidase-IV (DPPIV/CD26), NMR, surface plasmon resonance (SPR), and enzymatic assays demonstrate that reduced cleavage rates are a result of heparin-induced dimerization rather than direct association with the N terminus.

Our results suggest that heparin blocks the cardioprotective effect of CXCL12 by promoting dimerization. Heparin binds a site orthogonal to the dimer interface that partially overlaps the CXCR4 N terminus binding site and does not involve Lys-1. In principle, CXCL12 cardioprotection may be enhanced by modifications that alter its ability to self-associate or interact with heparin.

EXPERIMENTAL PROCEDURES

Protein Engineering, Expression, and Purification—CXCL12, $CXCL12_{H25R}$, and $CXCL12_2$ were expressed and purified as previously described (26, 32). All other chemokine variants were produced via mutagenesis of CXCL12 and $CXCL12_2$ constructs with complementary primers and the QuikChange site-directed mutagenesis kit (Stratagene) per the manufacturer's instructions. All expression vector inserts were confirmed by DNA sequencing.

Ex Vivo Cardioprotection Assay—Isolated hearts were perfused for 15 min, followed by aerobic perfusion 15 min prior to 30 min of global, no-flow ischemia, and 180 min of reperfusion. Aerobic perfusion including either 50 nM CXCL12, 50 units ml^{-1} heparin, or 50 nM CXCL12 plus 50 units ml^{-1} heparin. Hearts subjected to the above mentioned perfusion sequence in the absence of both CXCL12 and heparin served as ischemic controls. Hearts perfused continuously for 245 min served as nonischemic controls. Administration of the perfusion sequence, monitoring of cardiac function, and analysis of infarcted tissue was performed as previously described (19, 33, 34). Each dosage group consisted of four replicates. Resistance to injury from myocardial infarction/reperfusion was determined by a reduction in infarct size and/or an increase in recovery of developed pressure.

NMR Spectroscopy—NMR experiments were performed on a Bruker DRX 600 instrument equipped with a $^{1}H,^{15}N,^{13}C$ TXI-cryoprobe. Titration experiments were performed with either 50 μM [*U*-^{15}N]glymetCXCL12 or [*U*-^{15}N]glymetCXCL12$_2$ in 25 mM D-MES buffer (pH 6.8), 200 mM NaCl, 10% (v/v) D_2O, and 0.02% (w/v) NaN_3. CXCL12 and $CXCL12_2$ H^N assignments were transferred from previously published chemical shift tables (Biological Magnetic Resonance Bank identification code 16145 and 15633, respectively). Chemical shift perturbations were tracked using CARA (35). HCCH-TOCSY spectra were collected on 0.4 mM [*U*-^{15}N,^{13}C]$CXCL12_2$, 25 mM D-MES buffer (pH 6.8), 200 mM NaCl, 10% (v/v) D_2O, and 0.02% (w/v) NaN_3 in the presence of 0.0, 0.3, and 0.6 mM heparin decasaccharide of degree of polymerization (dp)10. Partial $CXCL12_2$

side chain assignments were transferred from previously published chemical shift table (Biological Magnetic Resonance Bank identification code 15633), and complete assignments were achieved with three-dimensional HCCH-TOCSY and three-dimensional ^{15}N-edited NOESY-HSQC. All of the experiments were performed at 298 K.

Binding site competition between $CXCR4_{1-38}$ and tetrasaccharide dp4 was assessed using ^{15}N HSQC experiments at 298 K. 200 μM $CXCR4_{1-38}$ was added to a sample comprised of 50 μM [*U*-^{15}N]$CXCL12_2$, 150 μM dp4, 25 mM D-MES, 200 mM NaCl, 10% (v/v) D_2O, and 0.2% (w/v) NaN_3.

Disaccharide and tetrasaccharide induced dimerization of CXCL12 were assessed using ^{15}N HSQC experiments at 298 K. A sample containing 10 μM [*U*-^{15}N,^{13}C]CXCL12, 25 mM D-MES (pH 6.8), 10% (v/v) D_2O, and 0.2% (w/v) NaN_3 was titrated with dp2 or dp4 (0, 5, 10, 20, and 30 μM).

Preparation of Heparin Biochip and SPR Analysis—The biotinylated heparin was immobilized to a streptavidin chip based on the manufacturer's protocol. The successful immobilization of biotinylated heparin was confirmed by the observation of a 250-resonance unit increase in the sensor chip. SPR measurements were performed on a BIAcore 3000 (GE Healthcare). The buffers were filtered and degassed prior to analysis. The protein samples were diluted in HBS-EP buffer (0.01 M HEPES, 150 mM NaCl, 3 mM EDTA, 0.005% surfactant P20, pH 7.4). Different dilutions of protein samples were injected at a flow rate of 30 μl min^{-1}. At the end of the sample injection, the same buffer was flowed over the sensor surface to facilitate dissociation. After a 3-min dissociation time, the sensor surface was regenerated by injecting 30 μl of 2 M NaCl. For competition with immobilized heparin, protein (50 nM) was mixed with certain concentrations of low molecular mass heparin ($dp_{avg}20$), heparin oligosaccharides (di (dp2), tetra (dp4), hexa (dp6), etc.) in HBS-EP buffer and injected over the heparin chip at a flow rate of 30 μl min^{-1}. For receptor competition studies, $CXCL12_2$ (50 nM) was premixed with $CXCR4_{1-38}$ (500 nM) and injected over the heparin chip. The response was monitored as a function of time at 298 K.

Fluorescence Polarization Assay—Fluorescence polarization assays were performed on a fluorometer (PTI) equipped with automated polarizers at 298 K. Titrations were conducted by monitoring the intrinsic tryptophan fluorescence polarization as a function of CXCL12 variant concentration in 100 mM $NaPO_4$ (pH 7.4), using emission and excitation wavelengths of 283 and 325 nm, respectively. All of the samples were filtered and degassed prior to analysis. The dimerization equilibrium dissociation constants (K_d) were determined by fitting polarization data as previously described (26).

Tissue Culture—THP-1 monocytes were obtained from American Type Culture Collection. The cells were maintained at a density of 3×10^5 to 9×10^5 cells ml^{-1} in RPMI 1640 medium supplemented with 20 mM HEPES, 10% (v/v) fetal bovine serum, 1 mM sodium pyruvate, 100 units ml^{-1} penicillin, and 100 μg ml^{-1} streptomycin at 310 K with 5% CO_2.

Calcium Response Assay—The cells were washed twice and resuspended in 96-well format at 2×10^5 cells well^{-1} in assay buffer: Hanks' buffered saline solution, 20 mM HEPES (pH 7.4), 0.1% (w/v) BSA, and FLIPR Calcium4 dye (Molecular Devices) and then incubated for 1 h at 310 K with 5% CO_2. Fluorescence was measured at 310 K using a FlexStation3 Microplate Reader (Molecular Devices) with excitation and emission wavelengths at 485 and 515 nm, respectively. After a 20-s base-line measurement, 30 nM CXCL12 variants were added, and the resulting calcium response was measured for an additional 50 s. Calcium flux was normalized to the response of CXCL12 or $CXCL12_2$. The samples were prepared in quadruplicate ($n = 2$).

DPPIV/CD26 Cleavage Reaction—Recombinant human DPPIV/CD26 was purchased from R&D Systems. Degradation reactions ($n = 3$) were comprised of 0.2 ng μl^{-1} DPPIV/CD26, 10 μM CXCL12, 2 μM [*U*-^{15}N]CXCL12(3–68), and 25 mM Tris (pH 8) alone or in the presence of 36 μM heparin (dp2 or dp4). The reactions were performed at 297 K. At the indicated time points, 25-μl aliquots were quenched using UltraMicroSpin columns (Silica C18; Nestgroup, Inc.). The samples were washed with 0.1% TFA and then eluted in 70% acetonitrile, 0.1% TFA. The samples were then mixed 1:1 with sinapinic acid solution and spotted on a MALDI plate. Three spectra, each comprised of 100 laser shots, were collected for each sample using a Voyager-DE Pro MALDI-TOF spectrometer (PerSeptive Biosystems). The intensity of CXCL12(3–68) was normalized to the [*U*-^{15}N]CXCL12(3–68) internal standard. The normalized intensity at each time point was subtracted from 5, the maximum ratio of unlabeled/labeled CXCL12(3–68), and then the half-life was calculated using nonlinear regression (pro Fit; QuantumSoft).

RESULTS

Heparin Attenuates the Cardioprotective Effect of CXCL12—CXCL12 is a potential anti-ischemic drug that has been observed to decrease the amount of infarcted tissue and improve cardiac function when administered either pre- or post-myocardial infarction (12–14, 16, 18). We previously showed that CXCL12 cardioprotection is mediated by the monomeric species (19). The antithrombotic properties of heparin are well established and highlighted by its presence as a clinical mainstay for the treatment of myocardial infarction. Because soluble heparin binds to and promotes dimerization of the chemokine (25, 26) and inhibits cell migration *in vitro* (30), we hypothesized that this interaction would also attenuate CXCL12-mediated cardioprotection.

Using an isolated rat heart model of ischemia/reperfusion injury, the cardioprotective effect of CXCL12 was measured in the presence of medicinal heparin (average molecular mass = 14 kDa; $dp_{avg}42$) (36). Increased resistance to injury from myocardial ischemia/reperfusion was determined by a reduction in infarct size and/or increase in recovery of left ventricle diastolic pressure. Whereas CXCL12 (50 nM) significantly reduced both measures of ischemia/reperfusion injury in isolated buffer-perfused rat heart relative to untreated controls, inclusion of heparin sodium (50 units ml^{-1}) completely eliminated the cardioprotective effect of CXCL12 (Fig. 1). This suggests that in a clinical setting, co-administration of heparin could attenuate the therapeutic benefit of CXCL12, underscoring the value of the molecular details for this chemokine/GAG interaction.

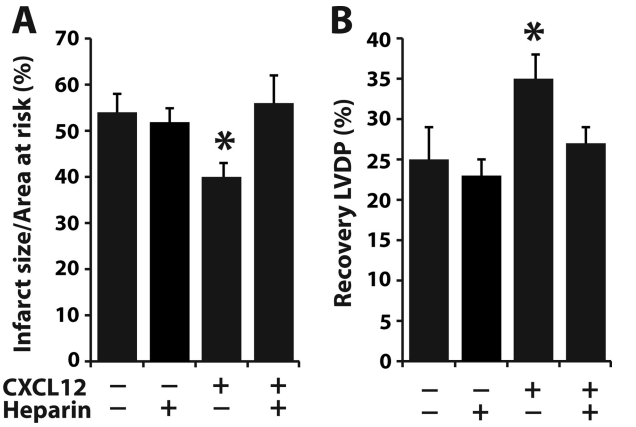

FIGURE 1. **Heparin eliminates CXCL12-mediated cardioprotection.** Isolated rat hearts ($n = 4$) were buffer-perfused for 15 min, followed by aerobic perfusion with either CXCL12 (50 nM) or CXCL12 (50 nM) in combination with medicinal heparin (50 units ml^{-1}) for an additional 15 min. The hearts were subjected to 30 min of no-flow global ischemia followed by 180 min of reperfusion. The percentage of infarct size and area at risk (*A*) and recovery left ventricle diastolic pressure (*LVDP*) (*B*) were measured in the left ventricle relative to nonischemic controls. The *asterisk* indicates statistical significance as determined by Student's *t* test. *A*, $p = 0.0006$. *B*, $p = 0.006$.

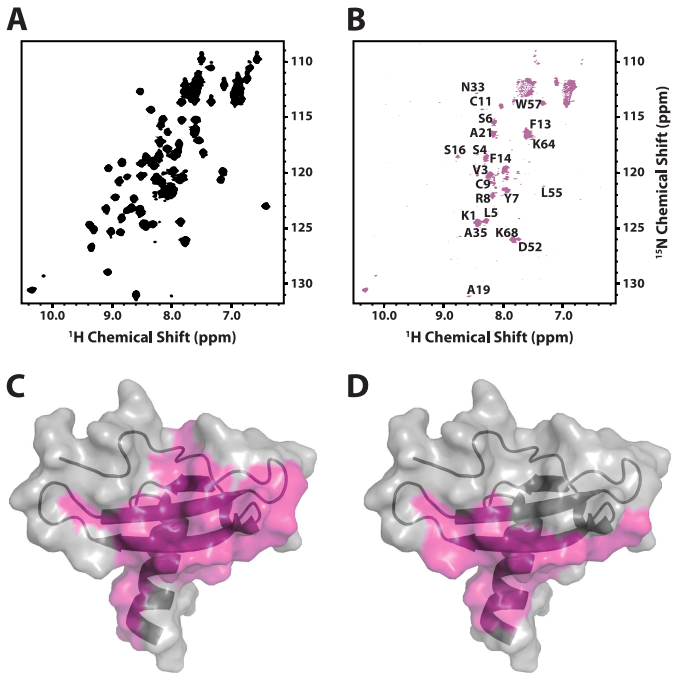

FIGURE 2. **Heparin dodecasaccharide produces extensive CXCL12 line broadening.** *A* and *B*, 50 μM ^{15}N-CXCL12 in the absence (*A*) and presence (*B*) of 150 μM dp12. Exchange broadening eliminated most signals at 0.5 equivalent of dp12. *C*, residues that exhibited extensive line broadening are colored *magenta* on the surface of CXCL12 (Protein Data Bank code 2KEE); broadening was observed in residues 15, 17–20, 23–29, 31, 37–42, 46, 48–51, 54–55, 58–63, 66, and 67. *D*, residues located at the dimer interface in the CXCL12 crystal structure (Protein Data Bank code 2J7Z) highlighted in *magenta* on the surface of CXCL12 (Protein Data Bank code 2KEE).

Heparin Dodecasaccharide Produces Substantial Line Broadening in CXCL12—Heparin-insensitive CXCL12 variants were identified by mutagenesis of the BBXB motif (residues 24–27) more than 10 years ago. Nonetheless, structural data on the binding interface is limited to a crystal structure of a heparin disaccharide bound to CXCL12 and NMR chemical shift data for a disaccharide and octasaccharide (30, 31). We monitored the binding of longer chain heparin oligosaccharides using two-dimensional ^{1}H-^{15}N HSQC NMR spectroscopy. Residues that exhibit large relative changes in chemical shift correlate with significant involvement in heparin binding—identifying the interface. Titration of 50 μM CXCL12 with increasing concentrations of heparin dodecasaccharide (0–150 μM) produced chemical shift changes and line broadening over a large area of the molecule including substantial perturbations clustered at the dimer interface (Fig. 2). Because heparin binding promotes CXCL12 dimerization (25, 26), we concluded that heparin-induced shifts arose from a combination of GAG-protein and protein-protein contacts.

High Affinity GAG Binding Requires CXCL12 Dimerization and Is Chain Length-dependent—To simplify analysis of the binding interaction by removing the monomer-dimer equilibrium, we tested whether the covalent dimer $CXCL12_2$ or preferential monomer $CXCL12_{H25R}$ are appropriate models for CXCL12-GAG binding (26, 32). SPR was used to measure the interaction of immobilized porcine intestinal heparin (average molecular mass = 14 kDa; dp_{avg} 42) with CXCL12, $CXCL12_{H25R}$, and $CXCL12_2$ (Table 1). Our results indicate that both monomeric and dimeric CXCL12 bind heparin but exhibit different rates of association and dissociation. Not surprisingly, dimeric $CXCL12_2$ binding is 200 times stronger than monomeric $CXCL12_{H25R}$. Wild type CXCL12 binds with an intermediate affinity that presumably reflects the relative contributions of monomers and dimers in equilibrium.

Next, we used SPR to measure the ability of immobilized heparin to displace CXCL12 from soluble heparin fragments of varying length. CXCL12 variants (50 nM) and various oligosaccharides (dp2 to dp20) were premixed and presented to immobilized heparin (average molecular mass = 14 kDa; dp_{avg}42). Supplemental Fig. S1 illustrates the changes in response units as a function of heparin concentrations that were used to calculate the IC_{50} and K_i values (Table 2). For CXCL12 and $CXCL12_{H25R}$, little or no displacement occurred for complexes with dp2, dp4, dp6, and dp8 heparin, but dp10 and longer oligosaccharides reduced binding to the immobilized heparin. The dp20 produced a sharp change in CXCL12 and $CXCL12_{H25R}$ response units characteristic of a change in complex stoichiometry. This is consistent with longer heparin chains increasingly promoting dimerization (25). It is also possible that dp20 may induce higher order oligomerization. The similar response of $CXCL12_{H25R}$ to wild type is consistent with its 10-fold weaker dimerization affinity (26). In contrast to CXCL12 and $CXCL12_{H25R}$, the affinity of $CXCL12_2$ for heparin increases in direct proportion to oligosaccharide length. $CXCL12_2$ had the tightest binding affinity and its association with the immobilized heparin was reduced the greatest by soluble heparin, regardless of size.

TABLE 1
Summary of kinetic data for interactions of heparin and CXCL12 variants

Variant	k_{on}	k_{off}	K_d
	$M^{-1}\,s^{-1}$	s^{-1}	M
CXCL12	4.90×10^6	1.50×10^{-1}	3.06×10^{-8}
$CXCL12_2$	7.60×10^5	3.80×10^{-3}	5.00×10^{-9}
$CXCL12_{H25R}$	1.19×10^5	2.50×10^{-2}	2.10×10^{-7}

TABLE 2
IC_{50} and K_i values calculated from SPR competition binding experiments

Competitor	CXCL12		$CXCL12_2$		$CXCL12_{H25R}$	
	IC_{50}	K_i	IC_{50}	K_i	IC_{50}	K_i
dp2	>10 μM	>3.8 μM	>10 μM	>91 μM	>10 μM	>8.3 μM
dp4	>10 μM	>3.8 μM	>10 μM	>91 μM	>10 μM	>8.3 μM
dp6	>10 μM	>3.8 μM	>10 μM	>91 μM	>10 μM	>8.3 μM
dp8	>10 μM	>3.8 μM	>10 μM	>91 μM	>10 μM	>8.3 μM
dp10	>10 μM	>3.8 μM	~7 μM	~636 nM	>10 μM	>8.3 μM
dp12	~10 μM	~3.8 μM	1 μM	91.0 nM	>10 μM	>8.3 μM
dp16	2 μM	769 nM	400 nM	36.4 nM	2.5 μM	2.1 μM
dp20	150 nM	57.7 nM	200 nM	18.2 nM	250 nM	208 nM
Low molecular weight heparin	500 nM	192 nM	150 nM	13.6 nM	750 nM	625 nM
Heparin	100 nM	38.5 nM	75 nM	6.82 nM	150 nM	125 nM

Heparin Binds Perpendicular to the CXCL12 Dimer Interface—Based on SPR results, we speculated that NMR measurements of CXCL12 binding to purified heparin oligosaccharides of varying length could provide useful structural details. To eliminate contributions from CXCL12 self-association and define chemical shift perturbations unambiguously caused by heparin binding, we used the constitutively dimeric $CXCL12_2$ variant. The titrations of various, heparin oligosaccharides of defined length (dp2, 4, 6, 8, 10, 12, 16, and 18) into CXCL12 were monitored by two-dimensional ^1H-^{15}N HSQC NMR experiments (supplemental Figs. S2–S4). As illustrated in Fig. 3*B*, the heparin tetrasaccharide (dp4) produced perturbations confined mainly to residues 23–30 (β1 strand), 35–43 (β2 strand), and 47–50 (β3 strand). Titration of heparin octasaccharide (dp8) induced corresponding shifts and additionally included residues 17–19 in the N-loop (Fig. 3*C*). Increasing the oligosaccharide length resulted in line broadening across the β-sheet and further extension of shift perturbations toward the helices of $CXCL12_2$ (Fig. 3*D*). The addition of 0.25 molar equivalents of octadecasaccharide (dp18) resulted in substantial sample precipitation, which precluded chemical shift mapping. However, the similar SPR response of dp16 and dp20 in the presence of $CXCL12_2$ suggests there are no substantial rearrangements of the binding interface at oligosaccharides greater than hexadecassacharide (dp16) (supplemental Fig. S1).

To identify specific interactions with positively charged side chains, we monitored changes in the HCCH-TOCSY of $CXCL12_2$ induced by heparin decasaccharide. The effects of heparin binding on each NMR signal were categorized as unaffected, perturbed, or exchange-broadened. Perturbed or exchange-broadened signals were assumed to identify residues proximal to the heparin-binding site. Fig. 3 illustrates the difference in HCCH-TOCSY signals for arginine (Fig. 3*E*) and lysine (Fig. 3*F*) residues in the absence and presence of 1.5 equivalents of dp10 heparin. The side chains of Arg-20, Arg-41, and Arg-47 display complete line broadening upon decasaccharide addition as expected from previous mutagenesis results (27, 30). Lys-24, Lys-27, and Lys-43 were also previously implicated in GAG binding (27, 28) and are similarly affected by dp10 binding.

The side chains of Arg-8 and Arg-12 display a mixture of perturbed and broadened resonances; the broadened H^{α}, H^{β}, and H^{γ} resonances and perturbed H^{δ} suggest a nominal contribution by the guanidinyl groups. Lys-54, Lys-56, and Lys-64 had varying degrees of incomplete broadening in H^{α}, H^{β}, H^{γ}, and H^{δ} with no perturbation in H^{ϵ}, suggesting no direct role in heparin binding through the primary amine. Consistent with the Lys-68 H^N resonance in the presence of all oligosaccharides tested, the side chain nuclei do not respond to decasaccharide and appear to be uninvolved in heparin binding.

Dissecting the Contribution of CXCL12 Residues to Dimerization and Heparin Binding—Several CXCL12 variants have been produced with mutations in Lys-24, Lys-27, or both that have a diminished affinity for heparin while retaining the ability to bind the CXCR4 receptor, promote calcium flux, and induce cell migration (27, 28). Because these residues are located in the β1-strand along the dimer interface, we hypothesized that either the mutations directly affect heparin binding or they inhibit dimerization and, indirectly, heparin binding. Fluorescence polarization was used to measure the dimerization dissociation constant of CXCL12(K24S), CXCL12(K27S), and CXCL12(K24S/K27S) (supplemental Fig. S5). The CXCL12(K27S) variant had a $K_d = 131 \pm 28$ μM similar to measurements for CXCL12 ($K_d = 140 \pm 19$ μM (26)), whereas CXCL12(K24S) and CXCL12(K24S/K27S) exhibited a reduced ability to dimerize with $K_d = 432 \pm 92$ and 327 ± 76 μM, respectively. To directly assess the effect of each substitution on heparin binding, we introduced the K24S, K27S, and K24S/K27S mutations into $CXCL12_2$ and measured the binding affinity to immobilized heparin (average molecular mass = 14 kDa; $dp_{avg}42$) using SPR (Table 3). Neither the single mutants nor the K24S/K27S variant reduced the $CXCL12_2$ binding affinity by more than 2-fold. This stands in stark contrast to the >1,000-fold change in affinity the mutations produce in the wild type CXCL12 background and underscores the importance of dimerization in heparin binding.

Analysis of our NMR titration data suggests a key role for Lys-27, Arg-41, and Arg-47 in heparin binding. Mutagenesis studies were undertaken to measure the contributions of these residues in direct heparin binding by producing alanine mutants in both the CXCL12 and $CXCL12_2$ background. As illustrated in supplemental Fig. S6, the function of each variant was confirmed via measurement of the calcium flux response. Mutations in the $CXCL12_2$ background report only on heparin binding, whereas the affinity of CXCL12 background mutants reflects both direct and indirect effects. The binding affinity of each mutant for immobilized heparin (average molecular mass = 14 kDa; $dp_{avg}42$) was determined by SPR (Table 3). In the CXCL12 background, single or multiple amino acid substitutions produce substantial changes in affinity. In contrast, single and double residue substitutions have little effect on $CXCL12_2$ binding: mutagenesis of all three basic residues is necessary to significantly reduce heparin binding. These results

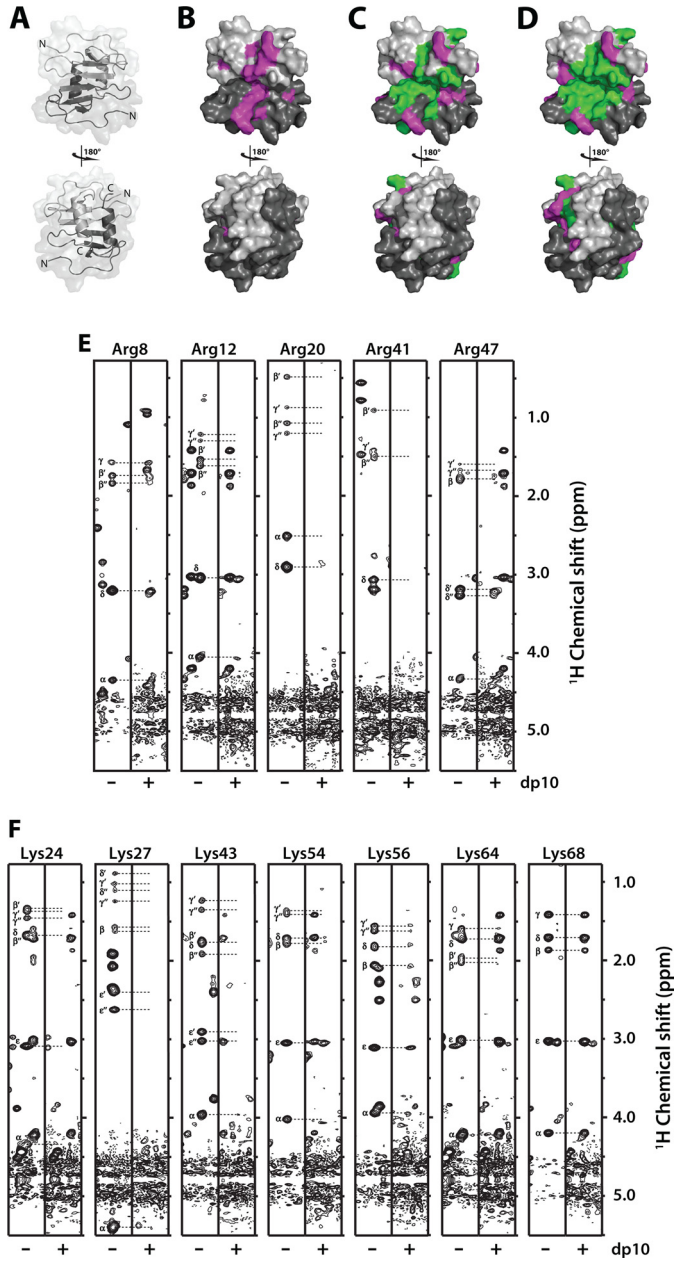

FIGURE 3. **Heparin binds orthogonal to the CXCL12 dimer interface in a size-dependent manner.** *A*, $CXCL12_2$ ribbon and surface representation in the absence of heparin; the two protomers are shaded in *light* and *dark gray* (N-terminal residues 1–8 are absent for ease of viewing). *B–D*, CXCL12 surface illustration in the presence of 3 equivalents of dp4 (*B*), dp8 (*C*), and dp12 (*D*). Residues that experience substantial chemical shift perturbations (*magenta*) and complete line-broadening (*green*) are mapped onto the $CXCL12_2$ NMR structure (Protein Data Bank code ID 2K01). *E* and *F*, HCCH-TOCSY H^{α} strips of all $CXCL12_2$ arginine (*E*) and lysine (*F*) residues in the absence and presence of heparin decasaccharide. Side chain correlations are labeled, and a *dashed line* indicates the positions of apo-$CXCL12_2$ resonances. Strong resonances near the Arg-47 H^{δ} peak in the presence of heparin are signals from Arg-8 that bleed through from a neighboring plane of the three-dimensional spectrum.

are consistent with a model in which clusters of positively charged side chains in two CXCL12 monomers join to form an elongated heparin-binding site that crosses the six-stranded β sheet of a CXCL12 dimer.

The Heparin Interface Partially Overlaps the CXCR4 N-terminal Binding Site—CXCR4-mediated cell migration is presumed to require that GAG-immobilized CXCL12 oligomers in the extracellular matrix be presented to the receptor, which transmits the external migratory signal to the internal cellular machinery. The initial interaction with CXCR4 is mediated through the receptor N terminus; however, inconsistencies exist as to whether this binding site overlaps with that of heparin (28, 30). The heparin-binding surface defined by chemical shift mapping is shared with the receptor-binding surface defined in structural studies with CXCR4 N-terminal peptides, including key sulfotyrosine binding residues Arg-47 and Lys-27 (32, 37). We tested the ability of an unsulfated CXCR4 N-terminal peptide comprising the first 38 amino acids, $CXCR4_{1-38}$, to either displace dp4 or form a ternary complex by binding simultaneously to a complementary site. Addition of $CXCR4_{1-38}$ had essentially no effect on the HSQC spectrum of dp4-bound $CXCL12_2$ (Fig. 4, *A* and *B*), demonstrating that heparin competes effectively with CXCR4 for CXCL12 binding. Using SPR, we tested whether the large chain immobilized heparin oligosaccharides (average molecular mass = 14 kDa; $dp_{avg}42$) could compete $CXCL12_2$ from $CXCR4_{1-38}$. As illustrated in Fig. 4*C*, $CXCL12_2$ (50 nM) preincubated with $CXCR4_{1-38}$ (500 nM) was unable to bind the immobilized heparin despite a 1000-fold higher affinity for the heparin.

TABLE 3
Summary of SPR kinetic data from the interaction of CXCL12 variants with heparin (average molecular mass = 14 kDa; $dp_{avg}42$)

	k_{on}	k_{off}	K_d
	$M^{-1}\,s^{-1}$	s^{-1}	M
$CXCL12_2$ variants			
$CXCL12_2$	7.6×10^5	3.8×10^{-3}	5.0×10^{-9}
K27A	4.1×10^5	2.2×10^{-3}	5.4×10^{-9}
R41A	8.6×10^5	1.9×10^{-3}	2.2×10^{-9}
R47A	2.7×10^5	1.9×10^{-3}	7.0×10^{-9}
K27A/R41A	1.6×10^6	1.2×10^{-2}	7.5×10^{-9}
K27A/R47A	5.7×10^5	3.3×10^{-3}	5.8×10^{-9}
R41A/R47A	9.0×10^5	3.0×10^{-3}	3.3×10^{-9}
K27A/R41A/R47A	5.2×10^2	3.7×10^{-3}	7.1×10^{-6}
K24S	2.2×10^5	2.8×10^{-3}	1.3×10^{-8}
K27S	6.2×10^5	2.1×10^{-3}	3.4×10^{-9}
K24S/K27S	7.0×10^5	7.2×10^{-3}	1.0×10^{-8}
Δ1–2	1.1×10^5	4.5×10^{-4}	4.1×10^{-9}
CXCL12 variants			
CXCL12	4.9×10^6	1.5×10^{-1}	3.1×10^{-8}
K27A	2.4×10^5	2.1×10^{-1}	8.8×10^{-7}
R41A	7.8×10^3	8.2×10^{-2}	1.1×10^{-5}
R47A	2.0×10^5	1.5×10^{-2}	7.5×10^{-8}
K27A/R41A	6.1×10^2	8.0×10^{-4}	1.3×10^{-6}
K27A/R47A	1.5×10^2	3.8×10^{-3}	2.5×10^{-5}
R41A/R47A	2.0×10^2	3.2×10^{-3}	1.6×10^{-5}
K27A/R41A/R47A	8.4×10^1	3.4×10^{-3}	4.0×10^{-5}
K24S	2.4×10^4	2.2×10^{-1}	9.2×10^{-6}
K27S	2.7×10^2	1.1×10^{-1}	4.1×10^{-4}
K24S/K27S	2.2×10^2	4.4×10^{-3}	2.0×10^{-5}
Δ1–2	2.5×10^5	2.4×10^{-2}	9.6×10^{-8}

Heparin Indirectly Protects the N Terminus from CD26/DPPIV Degradation—DPPIV/CD26 is a well known exopeptidase found in both a membrane-bound and a soluble form. It recognizes CXCL12 and cleaves between residues 2 and 3 to produce a truncated variant with a reduced affinity for, and an inability to activate, CXCR4 (38). Sadir *et al.* (29) used Western blot analysis to demonstrate that heparin molecules of increasing chain length protected CXCL12 from DPPIV/CD26-mediated degradation and attributed this effect to the direct association of heparin with Lys-1. To detect the participation of Lys-1 in the $CXCL12_2$/heparin interaction, we monitored dp10-induced chemical shift perturbations by HCCH-TOCSY. Although

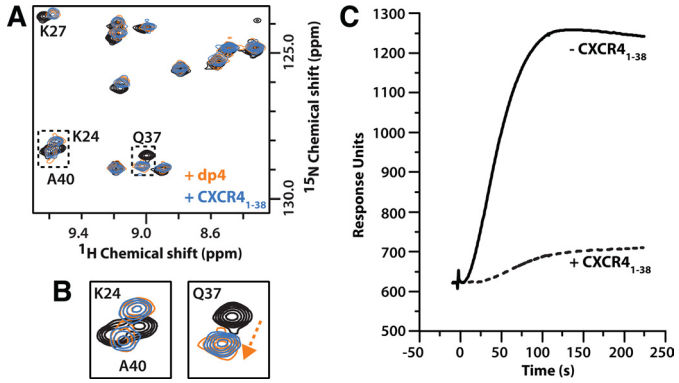

FIGURE 4. **The CXCR4$_{1-38}$ and heparin-binding sites overlap.** *A*, addition of CXCR4$_{1-38}$ peptide fails to disrupt the CXCL12$_2$-dp4 complex. Spectra for 50 μM CXCL12$_2$ (*black*), 50 μM CXCL12$_2$ + 150 μM dp4 (*orange*), and 50 μM CXCL12$_2$ + 150 μM dp4 + 200 μM CXCR4$_{1-38}$ (*blue*) are overlaid. *B*, close-up views of HSQC signals highlighted in *A*, showing that peaks shift upon dp4 binding but are unperturbed by the addition of CXCR4$_{1-38}$ peptide. *C*, 50 nM CXCL12$_2$ in the presence (*dashed line*) or absence (*solid line*) of 500 nM CXCR4$_{1-38}$ was injected over a heparin chip at a flow rate of 30 μl min^{-1}. An increase in response units is indicative of binding to the heparin chip.

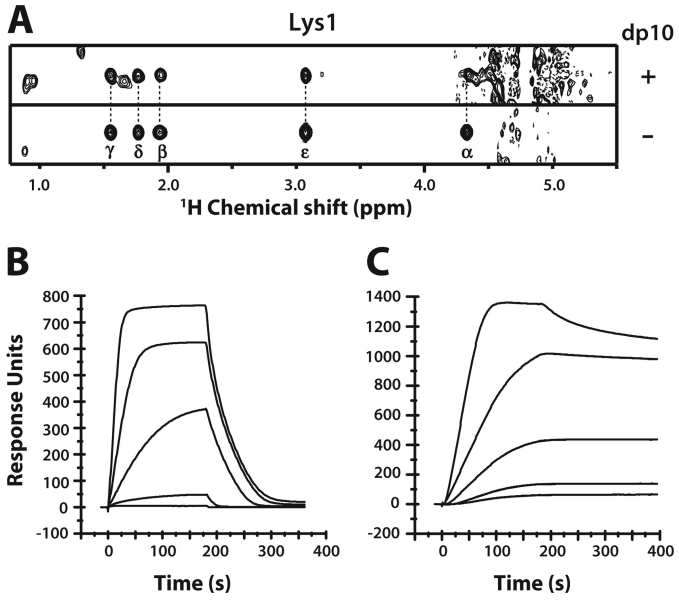

FIGURE 5. **Heparin does not interact with the CXCL12$_2$ N termini.** *A*, HCCH-TOCSY H$^\alpha$ strip for Lys-1 of CXCL12$_2$ in the presence (*top panel*) and absence (*bottom panel*) of heparin decasaccharide. Side chain correlations are labeled, and a *dashed line* indicates the positions of apo-CXCL12$_2$ resonances. *B* and *C*, SPR sensorgrams of 8, 16, 32, 63, and 125 nM CXCL12(3–68) (*B*) and CXCL12$_2$(3–68) (*C*) injected over a heparin chip at a flow rate of 30 μl min^{-1}. An increase in response units is indicative of binding to the heparin chip.

dodecasaccharides or larger were previously reported necessary for binding Lys-1 (29), our HSQC analysis attests the CXCL12 N-terminal residues 1–8 are similarly perturbed by dp10 and dp12; therefore, the decasaccharide was chosen as a compromise between sufficient oligosaccharide length and improved solubility. As illustrated in Fig. 5*A*, the sharp resonances of Lys-1 nuclei and residues 2–7 (data not shown) indicate little role for the primary amine or N terminus in oligosaccharide binding. Similarly, deletion of residues 1 and 2 (Δ1–2) from either CXCL12 or CXCL12$_2$ had no effect on binding long chain heparin by SPR (Fig. 5, *B* and *C*, and Table 3).

We recently demonstrated that the half-life of the CXCL12$_2$ N terminus is 25-fold greater than CXCL12 in the presence of

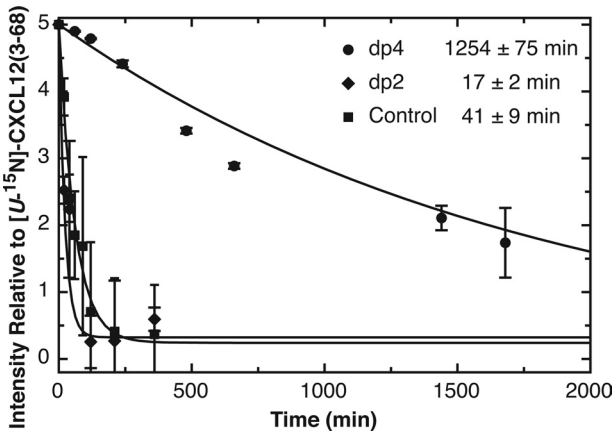

FIGURE 6. **Heparin protects the CXCL12 N terminus from CD26/DPPIV degradation by promoting dimerization.** 10 μM CXCL12 and 2 μM [U-^{15}N]CXCL12(3–68) was incubated with 0.2 ng μl^{-1} DPPIV/CD26 in the absence (*squares*) or presence of 36 μM dp2 (*diamonds*) or dp4 (*circles*). At the indicated time points, samples were desalted, mixed with sinapinic acid, and spotted onto a MALDI-TOF plate. The intensity of CXCL12(3–68) product formation was normalized to the [U-^{15}N]CXCL12(3–68) internal standard. The intensities at each time point were subtracted from 5, the maximum ratio of unlabeled to labeled CXCL12(3–68), and fitted to the half-life equation.

DPPIV/CD26 (39) and therefore hypothesized that heparin may indirectly protect Lys-1 by promoting CXCL12 dimerization. We incubated 10 μM CXCL12 and 0.2 ng μl^{-1} DPPIV/CD26 alone or in the presence of dp2 or dp4 heparin. The reaction was monitored by following CXCL12(3–68) product formation using MALDI-TOF MS (supplemental Fig. S7). Relative quantification was achieved by normalizing product intensities to a 2 μM [U-^{15}N]CXCL12(3–68) internal standard. Similar to our previous CXCL12 half-life of 26.5 ± 8.7 min (39), herein the buffer control exhibited a half-life of 41.5 ± 10 min. As shown in Fig. 6, protection of CXCL12 N-terminal cleavage is dependent on the size of heparin. Whereas dp2 does not provide protection ($\tau_{1/2}$ = 17.1 ± 2.4 min), dp4 slows the half-life to 1257 ± 75 min. The long term stability of DPPIV/CD26 was confirmed by measuring the half-life of CXCL12 degradation after 4 days (data not shown). The drastic difference in heparin-promoted dimerization between dp2 and dp4 is consistent with previous mass spectrometry studies at similar protein and oligosaccharide concentrations (25). We collected two-dimensional HSQC spectra at CXCL12 and heparin concentrations (dp2 and dp4) identical to those used in the DPPIV assay to look for signs of self-association (supplemental Fig. S8). Whereas dp2 induces little change in CXCL12, dp4 promotes chemical shift perturbations and line broadening consistent with dimerization.

DISCUSSION

Heparin is a well established antithrombotic agent and a clinical mainstay for the treatment of myocardial infarction. More recently, the anti-ischemic effects of CXCL12 have led to several novel treatment strategies. CXCL12 binds to soluble heparin and extracellular matrix GAGs. In the present study, we monitored the interaction of CXCL12 with soluble heparin by several methods and defined a binding site that may also be relevant to immobilization in the extracellular matrix. Although interactions with cell surface GAGs are essential for

chemotactic cell migration, soluble GAGs can block chemokine activity. We hypothesized that simultaneous administration of chemokine and heparin would diminish the protective properties of CXCL12 rather than synergizing their individual beneficial effects. As predicted, co-administration inhibited the cardioprotective effect of CXCL12 in an isolated rat heart model. This model reports directly on the function of cardiac tissue. If recruitment of progenitor cells is critical to the cardioprotective mechanism, the effect of soluble heparin administration on chemotaxis is unclear. *In vitro* studies suggest that heparin would inhibit the migration of cells (30). Further, the effect of CXCL12 on heparin activity is completely unknown and warrants future exploration.

The interaction between CXCL12 and heparin has been the focus of five papers over the last 13 years. The original mutagenic characterization by Amara *et al.* (28) identified residues Lys-24, His-25, and Lys-27 at the dimer interface as a canonical BB*X*B heparin-binding motif that is distinct from the CXCR4 N-terminal binding site. In 2001, Arg-41 and Arg-43 were proposed as additional contributors to the heparin binding interface. In the proposed structural model, heparin bound along the CXCL12 dimer interface, primarily making contacts with the β1-strand of each protomer (27). Later, a crystal structure of CXCL12 in complex with a heparin disaccharide analog identified two distinct binding sites: one high affinity site at the dimer interface and a second site between the N-loop region and the C-terminal helix (30). Finally, Sadir *et al.* (29) further expanded the proposed binding site to include the N termini; they concluded that the direct interaction of Lys-1 with heparin was responsible for limited proteolysis by DPPIV/CD26. Despite the wealth of data published on this crucial interaction, there are several inconsistencies in the predicted binding mode.

CXCL12/Heparin Interface—The monomer-dimer equilibrium and lack of data using long chain heparin molecules has significantly hindered the structural characterization of CXCL12-heparin complexes. We used the $CXCL12_2$ dimer to eliminate complications from CXCL12 self-association and monitor interactions with isolated heparin molecules ranging in size from dp2 to dp20. Whereas titration of heparin dodecasaccharide into wild type CXCL12 produced substantial line broadening throughout the dimer interface, $CXCL12_2$ enabled visualization of heparin-specific contacts. Our results differ from previous structural models. Instead of an interface mostly comprising the β1 strands and N terminus of each protomer in a dimer (Fig. 7*A*) (27, 29, 31), our data suggest that heparin drives dimer formation by interacting nearly orthogonal to the dimerization interface. We propose that the interface between CXCL12 and heparin crosses the entire six-stranded β-sheet, does not involve the N terminus, and is primarily mediated by Arg-20, Lys-24, Lys-27, Arg-41, Lys-43, and Arg-47 with the potential peripheral involvement of Arg-8 and Arg-12 (Fig. 7*B*).

A recently published model illustrated the octasaccharide-binding site more or less along the dimer interface; the terminal sugars interact with Arg-8 and Arg-12 on each protomer, whereas the core saccharides contact Lys-24, His-25, Lys-27, and Arg-41 (31). Although both Arg-8 and Arg-12 exhibit modest ^{1}H-^{15}N chemical shift perturbations and broadening of H^{α}, H^{β}, and H^{γ} resonances, the H^{δ} spins are minimally perturbed

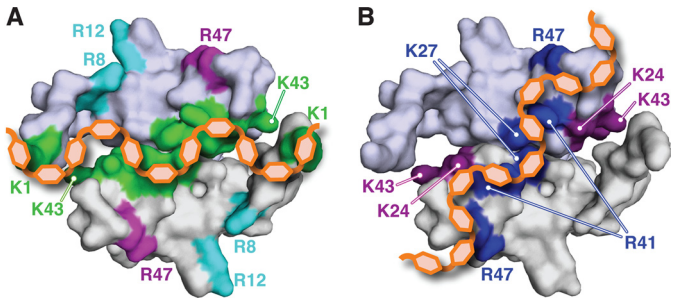

FIGURE 7. **Schematic representation of the heparin-CXCL12 binding mode.** *A*, the previously published binding mode proposed that heparin (*orange*) associates with CXL12 (*gray*) along the dimerization interface, primarily contacting the β1 strands and the Lys-1 residue of each protomer. Residues highlighted on the CXCL12 surface were identified in previous studies by Lortat-Jacob and co-workers (27–29) (*green*), Lolis and co-workers (30) (*magenta*), and Laguri *et al.* (31) (*cyan*). *B*, our combined biophysical analyses support a new model in which heparin promotes CXCL12 dimerization by contacting residues along the entire six-stranded sheet. The *highlighted* CXCL12 residues associate with heparin as determined by two-dimensional NMR, mutagenesis, SPR (*blue*), and three-dimensional NMR (*purple*).

and indicate little role for the guanidinyl groups in heparin binding. These results are consistent with previous R8E/R12E mutations that actually increased CXCL12 affinity for low molecular weight heparin (30). Perhaps removal of Arg-8 and Arg-12 enhances the interaction between heparin and basic residues in the chemokine cleft formed by the N-loop and β3 strand.

It should also be noted that the biological role for chemokine/GAG interactions is varied and context-dependent. Although there is a possibility that heparin and heparan sulfate recognize distinct binding sites, the similarity of their oligosaccharide structures and the inhibitory effect of heparin *in vivo* suggest that they share a single, overlapped binding site. At the same time, there may be important differences in the contributions of individual amino acid or glycan residues to the interaction. Our studies have identified residues that are likely to be involved in binding endogenous GAGs, but the unique structural features of heparin (*i.e.*, greater charge density compared with heparan sulfate and other extracellular matrix GAGs) may lead to slight differences in their binding modes.

Heparin and CXCR4 Sites Overlap—Previous analyses disagree as to whether the heparin and CXCR4 binding sites overlap (28, 30). Using a N-terminal peptide of CXCR4, we directly demonstrate competition between the receptor and heparin. The inability of the CXCR4 receptor peptide to dissociate dp4 does not prove that a native N terminus would also be insufficient. The CXCR4 N terminus can be *O*-sulfated at three tyrosine residues that together increase complex affinity from 4.5 $\pm$ 2.2 to 0.2 $\pm$ 0.2 μM (40). However, our results suggest that some of the surfaces occupied by CXCR4 sulfotyrosines may also be utilized for recognition of the sulfate moieties decorating GAG molecules. Considering the structural similarity between heparin and endogenous heparan sulfate, we speculate that similar competition occurs *in vivo*.

CXCL12 N Terminus Does Not Bind Heparin—The initial characterization of GAG binding excluded a role for Lys-1, as an antibody specific to the Lys-1–Pro-2 dipeptide was able to recognize CXCL12 bound to cell surface heparin (28). However, the same antibody was later used to show that heparin

molecules equal to and larger than dp12 compete for the N terminus (29). Our measurements of side chain chemical shift perturbations and SPR analysis of CXCL12(3–68) and $CXCL12_2$(3–68) clearly demonstrate that Lys-1 plays no role in binding to heparin oligosaccharides. Consequently, we concluded that heparin-mediated protection of the CXCL12 N terminus from proteolysis must be an indirect effect related to the GAG-induced oligomerization.

Dimerization Inhibits CXCL12 Degradation—DPPIV/CD26 is a multidomain enzyme that possesses distinct recognition and catalytic regions (41). To study the enhanced serum stability of $CXCL12_2$ compared with CXCL12, we recently monitored *in vitro* degradation by DPPIV/CD26 (39). The half-life of dimeric CXCL12 is 25-fold greater than wild type (39). Because oligosaccharide-induced dimerization is chain length-dependent, we hypothesized that heparin may possess a similar size-mediated influence on protection of DPPIV/CD26 degradation. Whereas incubation of CXCL12 with dp2 had no effect on degradation, dp4 delayed N-terminal cleavage nearly 30-fold. The lack of structural data for DPPIV/CD26 in complex with protein substrates makes the mechanism of enhanced stability unclear. The simplest explanation is the potential for overlap between the DPPIV/CD26 binding site and the CXCL12 dimerization interface. Most DPPIV/CD26 substrates are compact peptides with molecular masses less than 10 kDa (42). The large, dimeric CXCL12 may therefore also prevent the dimerization of DPPIV/CD26, which has been shown to reduce k_{cat} 30-fold (43). Matrix metalloprotease-2 also degrades $CXCL12_2$ slower than CXCL12 (39). Together, this suggests that heparin may indirectly protect CXCL12 from numerous other enzymes such as matrix metalloproteases 1, 3, 9, 13, and 14 (44), cathepsin G (45), and elastase (46). Because of growing clinical attention, it will be of interest to identify CXCL12 variants that maximize its cardioprotective properties while minimizing secondary interactions.

REFERENCES

1. Fuster, V., and Hurst, J. W. (2004) *Hurst's the Heart*, 11th Ed., McGraw-Hill, Medical Publishing Division, New York
2. Antman, E. M., Anbe, D. T., Armstrong, P. W., Bates, E. R., Green, L. A., Hand, M., Hochman, J. S., Krumholz, H. M., Kushner, F. G., Lamas, G. A., Mullany, C. J., Ornato, J. P., Pearle, D. L., Sloan, M. A., Smith, S. C., Jr., Alpert, J. S., Anderson, J. L., Faxon, D. P., Fuster, V., Gibbons, R. J., Gregoratos, G., Halperin, J. L., Hiratzka, L. F., Hunt, S. A., and Jacobs, A. K. (2004) ACC/AHA guidelines for the management of patients with ST-elevation myocardial infarction–Executive summary. A report of the American College of Cardiology/American Heart Association Task Force on Practice Guidelines (Writing Committee to Revise the 1999 Guidelines for the Management of Patients With Acute Myocardial Infarction). *Circulation* **110,** 588–636
3. Rosenberg, R. D., and Damus, P. S. (1973) The purification and mechanism of action of human antithrombin-heparin cofactor. *J. Biol. Chem.* **248,** 6490–6505
4. Handel, T. M., Johnson, Z., Crown, S. E., Lau, E. K., and Proudfoot, A. E. (2005) Regulation of protein function by glycosaminoglycans—as exemplified by chemokines. *Annu. Rev. Biochem.* **74,** 385–410
5. Johnson, Z., Proudfoot, A. E., and Handel, T. M. (2005) Interaction of chemokines and glycosaminoglycans. A new twist in the regulation of chemokine function with opportunities for therapeutic intervention. *Cytokine Growth Factor Rev.* **16,** 625–636
6. Proudfoot, A. E. (2006) The biological relevance of chemokine-proteoglycan interactions. *Biochem. Soc. Trans.* **34,** 422–426
7. Nagasawa, T., Hirota, S., Tachibana, K., Takakura, N., Nishikawa, S., Kitamura, Y., Yoshida, N., Kikutani, H., and Kishimoto, T. (1996) Defects of B-cell lymphopoiesis and bone-marrow myelopoiesis in mice lacking the CXC chemokine PBSF/SDF-1. *Nature* **382,** 635–638
8. Burns, J. M., Summers, B. C., Wang, Y., Melikian, A., Berahovich, R., Miao, Z., Penfold, M. E., Sunshine, M. J., Littman, D. R., Kuo, C. J., Wei, K., McMaster, B. E., Wright, K., Howard, M. C., and Schall, T. J. (2006) A novel chemokine receptor for SDF-1 and I-TAC involved in cell survival, cell adhesion, and tumor development. *J. Exp. Med.* **203,** 2201–2213
9. Sierro, F., Biben, C., Martínez-Muñoz, L., Mellado, M., Ransohoff, R. M., Li, M., Woehl, B., Leung, H., Groom, J., Batten, M., Harvey, R. P., Martínez, A. C., Mackay, C. R., and Mackay, F. (2007) Disrupted cardiac development but normal hematopoiesis in mice deficient in the second CXCL12/SDF-1 receptor, CXCR7. *Proc. Natl. Acad. Sci. U.S.A.* **104,** 14759–14764
10. Zou, Y. R., Kottmann, A. H., Kuroda, M., Taniuchi, I., and Littman, D. R. (1998) Function of the chemokine receptor CXCR4 in haematopoiesis and in cerebellar development. *Nature* **393,** 595–599
11. Ma, Q., Jones, D., Borghesani, P. R., Segal, R. A., Nagasawa, T., Kishimoto, T., Bronson, R. T., and Springer, T. A. (1998) Impaired B-lymphopoiesis, myelopoiesis, and derailed cerebellar neuron migration in CXCR4- and SDF-1-deficient mice. *Proc. Natl. Acad. Sci. U.S.A.* **95,** 9448–9453
12. Hu, X., Dai, S., Wu, W. J., Tan, W., Zhu, X., Mu, J., Guo, Y., Bolli, R., and Rokosh, G. (2007) Stromal cell derived factor-1α confers protection against myocardial ischemia/reperfusion injury. Role of the cardiac stromal cell derived factor-1α CXCR4 axis. *Circulation* **116,** 654–663
13. Saxena, A., Fish, J. E., White, M. D., Yu, S., Smyth, J. W., Shaw, R. M., DiMaio, J. M., and Srivastava, D. (2008) Stromal cell-derived factor-1α is cardioprotective after myocardial infarction. *Circulation* **117,** 2224–2231
14. Proulx, C., El-Helou, V., Gosselin, H., Clement, R., Gillis, M. A., Villeneuve, L., and Calderone, A. (2007) Antagonism of stromal cell-derived factor-1α reduces infarct size and improves ventricular function after myocardial infarction. *Pflugers Arch.* **455,** 241–250
15. Segers, V. F., Tokunou, T., Higgins, L. J., MacGillivray, C., Gannon, J., and Lee, R. T. (2007) Local delivery of protease-resistant stromal cell derived factor-1 for stem cell recruitment after myocardial infarction. *Circulation* **116,** 1683–1692
16. Sasaki, T., Fukazawa, R., Ogawa, S., Kanno, S., Nitta, T., Ochi, M., and Shimizu, K. (2007) Stromal cell-derived factor-1α improves infarcted heart function through angiogenesis in mice. *Pediatr. Int.* **49,** 966–971
17. Koch, K. C., Schaefer, W. M., Liehn, E. A., Rammos, C., Mueller, D., Schroeder, J., Dimassi, T., Stopinski, T., and Weber, C. (2006) Effect of catheter-based transendocardial delivery of stromal cell-derived factor 1α on left ventricular function and perfusion in a porcine model of myocardial infarction. *Basic Res. Cardiol.* **101,** 69–77
18. Zhang, G., Nakamura, Y., Wang, X., Hu, Q., Suggs, L. J., and Zhang, J. (2007) Controlled release of stromal cell-derived factor-1α *in situ* increases c-kit+ cell homing to the infarcted heart. *Tissue Eng.* **13,** 2063–2071
19. Veldkamp, C. T., Ziarek, J. J., Su, J., Basnet, H., Lennertz, R., Weiner, J. J., Peterson, F. C., Baker, J. E., and Volkman, B. F. (2009) Monomeric structure of the cardioprotective chemokine SDF-1/CXCL12. *Protein Sci.* **18,** 1359–1369
20. Penn, M. S., Zhang, M., Deglurkar, I., and Topol, E. J. (2004) Role of stem cell homing in myocardial regeneration. *Int. J. Cardiol.* **95,** S23–S25
21. Abbott, J. D., Huang, Y., Liu, D., Hickey, R., Krause, D. S., and Giordano, F. J. (2004) Stromal cell-derived factor-1α plays a critical role in stem cell recruitment to the heart after myocardial infarction but is not sufficient to induce homing in the absence of injury. *Circulation* **110,** 3300–3305
22. Yamaguchi, J., Kusano, K. F., Masuo, O., Kawamoto, A., Silver, M., Murasawa, S., Bosch-Marce, M., Masuda, H., Losordo, D. W., Isner, J. M., and Asahara, T. (2003) Stromal cell-derived factor-1 effects on ex vivo expanded endothelial progenitor cell recruitment for ischemic neovascularization. *Circulation* **107,** 1322–1328
23. Hattori, K., Heissig, B., Tashiro, K., Honjo, T., Tateno, M., Shieh, J. H., Hackett, N. R., Quitoriano, M. S., Crystal, R. G., Rafii, S., and Moore, M. A. (2001) Plasma elevation of stromal cell-derived factor-1 induces mobilization of mature and immature hematopoietic progenitor and stem cells. *Blood* **97,** 3354–3360

24. Heissig, B., Hattori, K., Dias, S., Friedrich, M., Ferris, B., Hackett, N. R., Crystal, R. G., Besmer, P., Lyden, D., Moore, M. A., Werb, Z., and Rafii, S. (2002) Recruitment of stem and progenitor cells from the bone marrow niche requires MMP-9 mediated release of kit-ligand. *Cell* **109,** 625–637
25. Fermas, S., Gonnet, F., Sutton, A., Charnaux, N., Mulloy, B., Du, Y., Baleux, F., and Daniel, R. (2008) Sulfated oligosaccharides (heparin and fucoidan) binding and dimerization of stromal cell-derived factor-1 (SDF-1/CXCL 12) are coupled as evidenced by affinity CE-MS analysis. *Glycobiology* **18,** 1054–1064
26. Veldkamp, C. T., Peterson, F. C., Pelzek, A. J., and Volkman, B. F. (2005) The monomer-dimer equilibrium of stromal cell-derived factor-1 (CXCL 12) is altered by pH, phosphate, sulfate, and heparin. *Protein Sci.* **14,** 1071–1081
27. Sadir, R., Baleux, F., Grosdidier, A., Imberty, A., and Lortat-Jacob, H. (2001) Characterization of the stromal cell-derived factor-1α-heparin complex. *J. Biol. Chem.* **276,** 8288–8296
28. Amara, A., Lorthioir, O., Valenzuela, A., Magerus, A., Thelen, M., Montes, M., Virelizier, J. L., Delepierre, M., Baleux, F., Lortat-Jacob, H., and Arenzana-Seisdedos, F. (1999) Stromal cell-derived factor-1α associates with heparan sulfates through the first β-strand of the chemokine. *J. Biol. Chem.* **274,** 23916–23925
29. Sadir, R., Imberty, A., Baleux, F., and Lortat-Jacob, H. (2004) Heparan sulfate/heparin oligosaccharides protect stromal cell-derived factor-1 (SDF-1)/CXCL12 against proteolysis induced by CD26/dipeptidyl peptidase IV. *J. Biol. Chem.* **279,** 43854–43860
30. Murphy, J. W., Cho, Y., Sachpatzidis, A., Fan, C., Hodsdon, M. E., and Lolis, E. (2007) Structural and functional basis of CXCL12 (stromal cell-derived factor-1α) binding to heparin. *J. Biol. Chem.* **282,** 10018–10027
31. Laguri, C., Sapay, N., Simorre, J. P., Brutscher, B., Imberty, A., Gans, P., and Lortat-Jacob, H. (2011) ^{13}C-Labeled heparan sulfate analogue as a tool to study protein/heparan sulfate interactions by NMR spectroscopy. Application to the CXCL12α chemokine. *J. Am. Chem. Soc.* **133,** 9642–9645
32. Veldkamp, C. T., Seibert, C., Peterson, F. C., De la Cruz, N. B., Haugner, J. C., 3rd, Basnet, H., Sakmar, T. P., and Volkman, B. F. (2008) Structural basis of CXCR4 sulfotyrosine recognition by the chemokine SDF-1/CXCL12. *Sci. Signal.* **1,** ra4
33. Baker, J. E., Curry, B. D., Olinger, G. N., and Gross, G. J. (1997) Increased tolerance of the chronically hypoxic immature heart to ischemia. Contribution of the KATP channel. *Circulation* **95,** 1278–1285
34. Baker, J. E., Konorev, E. A., Gross, G. J., Chilian, W. M., and Jacob, H. J. (2000) Resistance to myocardial ischemia in five rat strains. Is there a genetic component of cardioprotection? *Am. J. Physiol. Heart Circ. Physiol.* **278,** H1395–H1400
35. Keller, R. (2004) *The Computer Aided Resonance Assignment/Tutorial*, Cantina, Zurich, Switzerland
36. Zhang, F., Yang, B., Ly, M., Solakyildirim, K., Xiao, Z., Wang, Z., Beaudet, J. M., Torelli, A. Y., Dordick, J. S., and Linhardt, R. J. (2011) Structural characterization of heparins from different commercial sources. *Anal. Bioanal. Chem.* **401,** 2793–2803
37. Veldkamp, C. T., Seibert, C., Peterson, F. C., Sakmar, T. P., and Volkman, B. F. (2006) Recognition of a C*X*CR4 sulfotyrosine by the chemokine stromal cell-derived factor-1α (SDF-1α/CXCL12). *J. Mol. Biol.* **359,** 1400–1409
38. Crump, M. P., Gong, J. H., Loetscher, P., Rajarathnam, K., Amara, A., Arenzana-Seisdedos, F., Virelizier, J. L., Baggiolini, M., Sykes, B. D., and Clark-Lewis, I. (1997) Solution structure and basis for functional activity of stromal cell-derived factor-1. Dissociation of CXCR4 activation from binding and inhibition of HIV-1. *EMBO J.* **16,** 6996–7007
39. Takekoshi, T., Ziarek, J. J., Volkman, B. F., and Hwang, S. T. (2012) A locked, dimeric CXCL12 variant effectively inhibits pulmonary metastasis of CXCR4-expressing melanoma cells due to enhanced serum stability. *Mol. Cancer Ther.* **11,** 2516–2525
40. Seibert, C., Veldkamp, C. T., Peterson, F. C., Chait, B. T., Volkman, B. F., and Sakmar, T. P. (2008) Sequential tyrosine sulfation of CXCR4 by tyrosylprotein sulfotransferases. *Biochemistry* **47,** 11251–11262
41. Thoma, R., Löffler, B., Stihle, M., Huber, W., Ruf, A., and Hennig, M. (2003) Structural basis of proline-specific exopeptidase activity as observed in human dipeptidyl peptidase-IV. *Structure* **11,** 947–959
42. Boonacker, E., and Van Noorden, C. J. (2003) The multifunctional or moonlighting protein CD26/DPPIV. *Eur. J. Cell Biol.* **82,** 53–73
43. Chien, C. H., Huang, L. H., Chou, C. Y., Chen, Y. S., Han, Y. S., Chang, G. G., Liang, P. H., and Chen, X. (2004) One site mutation disrupts dimer formation in human DPP-IV proteins. *J. Biol. Chem.* **279,** 52338–52345
44. McQuibban, G. A., Butler, G. S., Gong, J. H., Bendall, L., Power, C., Clark-Lewis, I., and Overall, C. M. (2001) Matrix metalloproteinase activity inactivates the C*XC* chemokine stromal cell-derived factor-1. *J. Biol. Chem.* **276,** 43503–43508
45. Delgado, M. B., Clark-Lewis, I., Loetscher, P., Langen, H., Thelen, M., Baggiolini, M., and Wolf, M. (2001) Rapid inactivation of stromal cell-derived factor-1 by cathepsin G associated with lymphocytes. *Eur. J. Immunol.* **31,** 699–707
46. Valenzuela-Fernández, A., Planchenault, T., Baleux, F., Staropoli, I., Le-Barillec, K., Leduc, D., Delaunay, T., Lazarini, F., Virelizier, J. L., Chignard, M., Pidard, D., and Arenzana-Seisdedos, F. (2002) Leukocyte elastase negatively regulates Stromal cell-derived factor-1 (SDF-1)/CXCR4 binding and functions by N-terminal processing of SDF-1 and CXCR4. *J. Biol. Chem.* **277,** 15677–15689